Send Orders for Reprints to reprints@benthamscience.net

Current Radiopharmaceuticals, 2020, *13*, 1-06

RESEARCH ARTICLE

Diagnostic value of the early Heart-to-Mediastinum count ratio in Cardiac 123I-mIBG Imaging for Parkinson's Disease

Viviana Frantellizzi[1], Valentina Lavelli[2,*], Cristina Ferrari[3], Angela Sardaro[3], Alessio Farcomeni[4], Massimiliano Pacilio[5], Cristian Borrazzo[5,6], Roberto Pani[7], Giuseppe Rubini[2] and Giuseppe De Vincentis[6]

[1]Department of Molecular Medicine, Sapienza, "Sapienza" University of Rome, viale Regina Elena,324, 00161Rome, Italy; [2]Nuclear Medicine Unit, Interdisciplinary Department of Medicine – University of Bari "Aldo Moro", Bari, Italy; [3]Interdisciplinary Department of Medicine, Section of Radiology and Radiation Oncology, University of Bari "Aldo Moro", Bari, Italy; [4]Department of Economic and Finance, "Tor Vergata" University of Rome, via Columbia, 2, 00133Rome, Italy; [5]Department of Medical Physics, Azienda Ospedaliera Universitaria Policlinico Umberto I, viale del Policlinico 155, 00161Rome, Italy; [6]Department of Radiological Sciences, Oncology and Anatomical Pathology, Sapienza, "Sapienza" University of Rome, viale Regina Elena,324, 00161Rome, Italy; [7]Department of Sciences and Medico-Surgical Biotechnologies, "Sapienza" University of Rome, viale Regina Elena,324, 00161Rome, Italy

Abstract: ***Background*:** Early diagnosis of Parkinson's disease (PD) is of primary importance. The delayed (3-4 h after injection) Iodine-123-Metaiodobenzylguanidine (123I-mIBG) scintigraphy has been proven to be effective in early differential diagnosis for Lewy body disease. But early imaging (15-30 min after injection) has only been marginally studied for its possible diagnostic role. In this prospective study, a threshold for the early Heart-to-Mediastinum (H/M) count ratio has been investigated, obtaining a diagnostic accuracy analogous to conventional, delayed imaging.

***Methods*:** One hundred and eight patients with suspected Parkinson's disease (PD) were acquired after 15 and 240 minutes from the injection of 150-185 MBq of 123I-mIBG. The early and late H/M (He/Me and Hl/Ml) were evaluated by drawing Region-of-Interests on the heart and the upper half of the mediastinum. Optimal threshold (Youden index) and overall predictive performance were determined by receiver operating characteristic curve, classifying tentatively patients having an Hl/Ml lower than 1.6 as suffering from PD.

***Results*:** He/Me was not significantly different from Hl/Ml (p-value=0.835). The Area-under-curve was 0.935 (95%CI: 0.845-1.000). The He/Me optimal threshold was 1.66, with sensitivity, specificity, and diagnostic accuracy of 95.5%, 85.7, and 90.7%, respectively.

***Conclusion*:** The He/Me Ratio is almost as accurate as the widely used delayed 123I-mIBG imaging, reducing the burden of delayed imaging but preserving the diagnostic accuracy of the method. Moreover the differential diagnosis in Parkinson's disease can be made in just 25 minutes against the 4 hours currently needed, lowering costs of the healthcare system and improving patients compliance.

ARTICLE HISTORY

Received: March 30, 2020
Revised: June 10, 2020
Accepted: June 19, 2020

DOI:
10.2174/1874471013999200727211633

Keywords: Cardiac imaging, parkinson's disease, 123I-mIBG, planar imaging, heart-to-Mediastinum, lewy body disease.

1. INTRODUCTION

Early diagnosis of Parkinson's disease (PD) is of primary importance, as the symptoms of different types of neurodegenerative diseases frequently overlap, especially in the earlier stages at onset [1]. Meta-iodobenzylguanidine (mIBG), a guanethidine analog, shows an uptake mechanism and storage similar to that of noradrenaline. It is actively taken up by the postganglionic presynaptic nerve endings of the adrenergic nervous system. Therefore, 123I-mIBG cardiac scintigraphy can non-invasively assess the postganglionic presynaptic cardiac sympathetic nerve endings [2, 3]. Loss of cardiac MIBG uptake was demonstrated in Lewy body disease patients, such as PD [4] and dementia with Lewy bodies (DLB) [5]. Due to the characteristics, 123I-mIBG can increase the accuracy of the differential diagnosis for Lewy body disease (PD and DLB) from other parkinsonism and Alzheimer's disease. Uptake values are ~~abnormal~~ reduced specifically in PD relative to other neurodegenerative mov-

* Address correspondence to this author at the Nuclear Medicine Unit, Interdisciplinary Department of Medicine – University of Bari "Aldo Moro", Bari, Italy; Tel: +39 0805592779, Fax: +39 0805592983;
E-mail: valentina.lavelli@gmail.com

Table 1. Patient Characteristics

	Total (n=108)
Age (years); mean (SD)	64.3 (9.1)
Sex (male)	66.6%; n=72
Height (cm); mean (SD)	162.4 (9.7)
Weight (Kg); mean (SD)	68.7 (15.3)
Coronary artery disease	none
Diabetes mellitus	none
Hoehn e Yahr class	
1	62%; n=67
1.5	4-38%; n=41

ement disorders [4, 6]. Patients exhibit low uptake also with DLB, and this finding is considered a supportive feature of the current diagnostic criteria [7]. The reduction in myocardial uptake can be quantified by the Heart-to-Mediastinum (H/M) mean count ratio on 123I-mIBG scintigraphy. Most of the previous studies used the delayed (*i.e*., 3-4 hours after the administration) H/M ratio [8], but the diagnostic value of the early H/M ratio is often emphasized more and more [9-12]. Early imaging alone could reduce the burden imposed by delayed imaging on the patient. In this prospective study, we propose a basic methodology, to tune the threshold for early H/M ratio obtaining a diagnostic accuracy analogous to the better-consolidated practice of delayed imaging in PD patients.

2. MATERIAL AND METHODS

One hundred and eight patients (mean age 64.3±9.1 years) presenting Parkinsonism syndrome of recent onset (Hoehn and Yahr $\leq$ 1.5) were enrolled and submitted to 123I-mIBG scintigraphy. Exclusion criteria were diabetes mellitus and history of coronary artery disease. Neurologists performed the initial clinical evaluation after the onset of symptoms (mean 1.12 ± 0.78 years), with a difference, between first and follow-up visit, of the mean time of 3.32 ± 1.98 years. The follow-up assessment included both semi-structured interviews and neurological examinations, probed motor system and cerebellar function, postural stability and gait, clinical symptoms of autonomic nervous system function, cranial nerves, and sensation. A follow-up diagnosis of PD was made according to both Gelb *et al*. [13] and Gilman *et al*. diagnostic criteria [14]. Data analysis was then performed after at least three years of follow-up. Patients clinical characteristics are summarized in Table **1**. The study protocol was approved by the local ethics committee and conducted following the ethical standards laid down in the 1964 Declaration of Helsinki and its later amendments. Before the infusion of 150-185 MBq of 123I-mIBG (AdreView, GE Healthcare), a 5% Lugol solution was administered to block the thyroid uptake. Planar images were acquired after 15 and 240 minutes (early and late phase, respectively) from the injection, with a dual-head gamma camera (Infinia, GE Healthcare, Milwaukee, USA), using low-energy parallel-hole high resolution (LEHR) collimator and energy window centered at 159 KeV (±10% wide). Thorax anterior images were acquired for 10 min, with 128x128 matrix and zoom factor of 1. Immediately after the planar images, at 25 minutes and 250 minutes after injection, SPECT cardiac images were acquired with the dual-headed gamma camera over 18° using a 90°-rotation, starting at 45° right-anterior oblique projection and proceeding to the 45° left-posterior oblique projection. A 64x64 matrix was used for the SPECT studies (zoom factor 1). We applied a step-and-shot technique (64 projections, 30 seconds of duration per frame in non-gated mode).

2.1. Image Analysis

On planar images, polygonal Region-of-Interests (RoIs) were drawn manually on the heart (including the left ventricular cavity), whereas a 7x7 square ROI was placed on the upper half of the mediastinum (below the thyroid). ROIs were duplicated from the late to early images assuming the thyroid image as a fiducial marker, and H/M ratios in both phases (He/Me and Hl/Ml) were calculated as mean count per pixel in myocardium divided by that in the mediastinum. Using Myovaton software implemented on a Xeleris Duo platform (GE Healthcare), SPECT images were reoriented in short, vertical long, and horizontal long heart axes after filtered-back-projection (FBP) reconstruction. Heart images were analyzed with a standard 17-segments model similarly to the conventional methods used for myocardial perfusion imaging. All 17 segments were scored using a 5-point scale where myocardial 123I-mIBG uptake was expressed as a percentage of the maximum myocardial uptake. The reconstruction method is described elsewhere [15]. The defect scores were calculated as the sum of the segmental scores and the early and late summed scores (ESS and LSS, respectively) were obtained.

2.2. Statistical Analysis

Correlation between He/Me and Hl/Ml was investigated with the Spearman correlation coefficient and related test. Differences between He/Me and Hl/Ml were investigated through the Wilcoxon rank-sum test. Simple linear regression was used to assess calibration. The overall predictive performance of He/Me, as well as ESS and LSS, was investigated by Receiver Operating Characteristic (ROC) curve, classifying, in the case of He/Me, tentatively patients having an Hl/Ml lower than 1.6 as suffering from PD. The optimal threshold was selected by maximizing the sum of sensitivity and specificity (Youden index). The Youden index, defined as (sensitivity + specificity) − 1, was calculated at each cut-off point. The Threshold point which showed the highest Youden index was considered the optimal cut-off value [[16]]. Significance of AUC and confidence intervals were computed *via* the bootstrap. All analyses have been conducted with R software version 3.1.2.

3. RESULTS

The H/M ratios calculated on the early and late images did not show a normal distribution. The He/Me ranged from 1.2 to 2.2 (median 1.63), whereas the Hl/Ml from 1.0 to 2.44 (median 1.59). He/Me was not significantly different from Hl/Ml (p-value=0.835). Similarly, The SS calculated on the

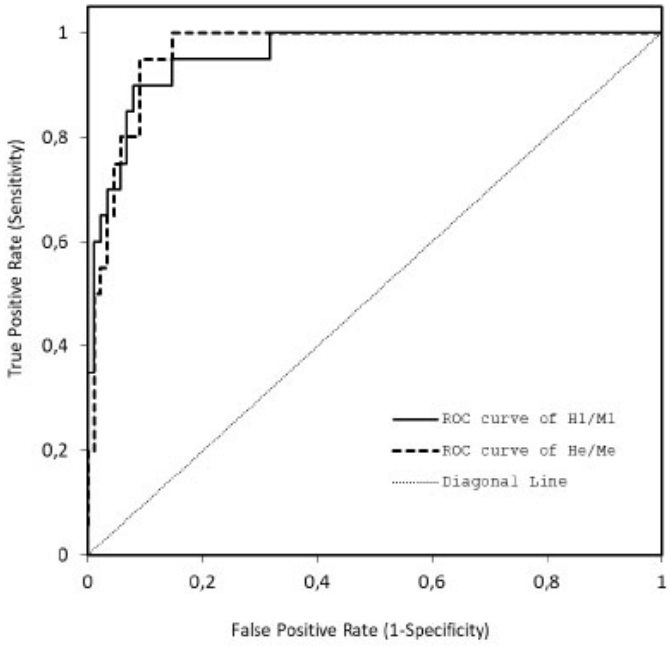

Fig. (1). ROC curve of the He/Me and Hl/Ml ratio to detect the disease, calculated ~~assuming~~ using different cut-off. (*A higher resolution / colour version of this figure is available in the electronic copy of the article*).

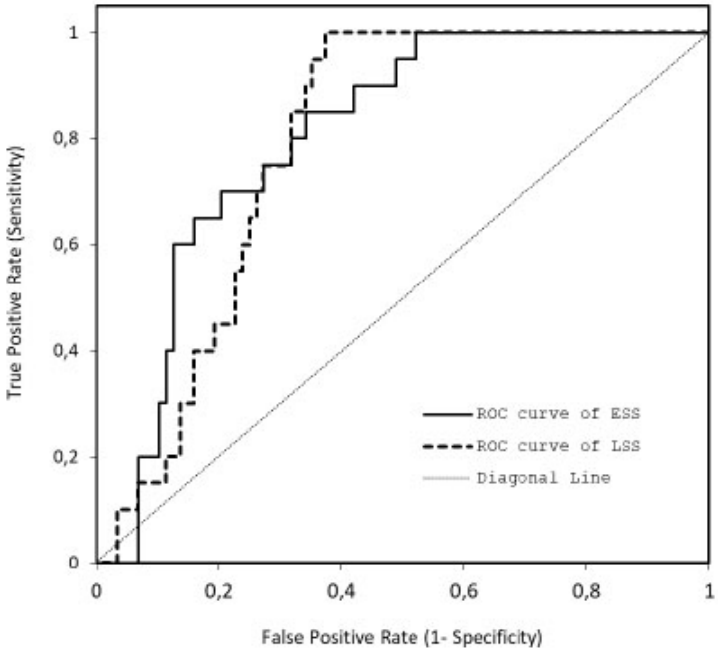

Fig. (2). ROC curve of the ESS and LSS to detect the disease, calculated ~~assuming~~ using different cut-off. (*A higher resolution / colour version of this figure is available in the electronic copy of the article*).

early and late images did not show a normal distribution. The ESS ranged from 0 to 67 (median 19), whereas the LSS from 2 to 68 (median 24). ESS was not significantly different from LSS (p-value=0.837). Analyzing the overall predictive performance of planar and SPECT parameters, the ROC curves in (Fig. **1**) (calculated assuming different cut-off) highlights that He/Me is highly reliable as Hl/Ml, in fact, ROC curve analysis showed an AUC of 0.972 ± 0.037 (95%

Table 2. Comparison of the area under the ROC curve (AUC) and optimal sensitivities and specificities of each parameter is shown in the associated table.

Parameters (1)	AUC (2)	SE (3)	95%CI (4)	Cutoff (5)	Sensitivity (6)	Specificity (7)	Accuracy (8)
He/Me	0.972	0.037	0.867-1.000	1.77	91.0%	95.0%	0.916
Hl/Ml	0.923	0.043	0.833-1.000	1.83	92.0%	90.0%	0.917
ESS	0.826	0.059	0.710-0.942	23	80.0%	68.2%	0.824
LSS	0.789	0.064	0.664-0.913	13	75.0%	73.0%	0.731

Columns show: (1) Parameters, (1) area under the curve (AUC), (3) Standard Error (SE), (4) Confidence Interval (CI) at 95% (5) optimal thresholds, (6) Sensitivity, (7) Specificity and (8) diagnostic accuracy.

Table 3. Columns show: (1) Comparison methods, (2) Mean Difference Relative (MDR) between AUC and (3) p-value. The statistical significance is achieved when p < 0.05*.

Comparison Methods	MDR (%)	p-value
He/Me vs ESS	17.7	0.043*
He/Me vs LSS	23.2	0.018*
Hl/Ml vs ESS	12.3	0.185
Hl/Ml vs LSS	17.0	0.083
He/Me vs Hl/Ml	5.3	0.392
ESS vs LSS	4.7	0.670

CI:0.867-1.000). With a He/Me threshold of 1.77, sensitivity was 91.0% and specificity 95.0%, with a diagnostic accuracy of 91.6%. As regards, Hl/Ml, as a result, we have found an AUC of 0.923 ± 0.043 (95%CI: 0.833-1.000). With a Hl/Ml threshold of 1.83, sensitivity was 92.0% and specificity 90.0%, with a diagnostic accuracy of 91.7%. As to the ROC curves in (Fig. **2**) highlights that ESS is reliable as LSS, ROC curve analysis showed an AUC of 0.826 ± 0.059 (95%CI: 0.710-0.942). With an ESS threshold of 23, sensitivity was 80.0% and specificity 68.2%, with a diagnostic accuracy of 82.4%. Finally, the AUC of LSS was 0.789 ± 0.0634 (95%CI: 0.664-0.913). With an LSS threshold of 13, sensitivity was 75.0% and specificity 73.0%, with a diagnostic accuracy of 73.1%. We report the values, obtained with the ROC curve analysis optimal thresholds in Table **2**. Table **3** shows the Mean Relative Difference (MRD) for each paired comparison of the methods. The MRD is defined as (A1-A2)/A2 where A1 is the AUC of the first method, while A2 is the AUC of the referred to the second method. The pair comparisons for which the AUC are statistically significant (t-test on averages, a threshold on p-value <0.05) are He/Me vs ESS and He/Me vs LSS.

4. DISCUSSION

The cardiac sympathetic function is frequently impaired even in the early stages of PD, suggesting early involvement of the cardiac sympathetic system [4, 17]. Moreover, the degeneration of the distal axons of the cardiac sympathetic nerve precedes loss of their mother neurons in the paravertebral sympathetic ganglia [18]. 123I-mIBG imaging represents a validated tool for the assessment of cardiac sympathetic innervation. However, there is still no universally accepted imaging protocol to conduct examinations. Various authors show methodological variability that involves injected activities (111 to 370 MBq), acquisition matrices (128x128 or 256x256 pixels), collimators (low energy or medium energy) [19, 20] and also the timing, that varied from 15 to 30 min for early imaging and 3 to 4 h for delayed phase of the study [21, 22]. Even the identification of accepted threshold values for H/M ratio on planar imaging to differentiate between normal and pathological subjects still represents an unresolved issue [23]. Recent studies on the DLB reported optimal thresholds of 2.0-2.2 for He/Me, and 2.27 for Hl/Ml as physiological ratio [11, 12]. Previous work on the PD reported 1.92 and 1.68 for He/Me and Hl/Ml [9], respectively, evidencing a slight difference between the two threshold values, and confirming that cardiac uptake is abnormal specifically in PD, as reported also elsewhere [4]. In this work, a cut-off value of 1.6 for Hl/Ml was tentatively assumed, coherently with studies on heart failure [24], resulting in a cut-off of 1.66 for He/Me. This threshold value, obtained using LEHR collimator, can be assumed equal to 2.98 according to Verschure *et al* [25]. Therefore, He/Me optimal threshold would be slightly higher than that of Hl/Ml. Since the information on the clinical use of the 123I-mIBG is still not satisfactory, especially from the point of view of the cardiac tomographic image, it was decided to acquire the SPECT images of these patients. However, the results obtained are not encouraging, in fact the diagnostic accuracy of the planar images is even higher. Furthermore, even the early SPECT images do not have a good diagnostic accuracy compared to the delayed ones. It has therefore been shown that the SPECT approach to date seems not only useless but also expensive in terms of time spent for the patient. In our opinion, the most important result of this study is represented by the ability of early imaging to provide results equivalent to those of late images, from a diagnostic point of view. It may lead to the shortening of imaging protocols in PD patients while maintaining the accuracy and precision of planar 123I-mIBG imaging parameters. In fact, as compared with the standardized late acquisition (240 min), the early acquisition is equivalent. Our results indicate the potential role of early imaging alone, without the need to wait for the 3-4 hours required for late acquisitions. It, in principle, may produce logistic advantages of Nuclear Medicine centers concerning PD patients [25]. The significant reduction in execution times can make this examination much easier for patients who often have reduced compliance. These considerations could make 123I-mIBG scan a diagnostic method of great efficacy and reliability easily applicable in often fragile patients. This approach could also be suitable for other types of patients with other indications, for example those

with heart failure or in general with cardiovascular disease. A limitation of the study is represented by the limited number of patients enrolled, and of course, it does not allow us to state conclusive considerations. These suggestions need to be validated through a large sample size. However, the possibility to simplify the diagnostic procedure deserves consideration and appears worthy of further, larger studies. A second limitation of the study is that of having to consider that, although this approach can be used for all patients in whom there is a suspicion of PD, some functional and / or pathological movement disorders could determine false positive results. This study demonstrates the possibility to tune effectively the He/Me threshold, basing on the most frequently used methodology of the delayed 123I-mIBG imaging, reducing sensibly the burden imposed by delayed imaging, while preserving diagnostic accuracy and allowing time and economic saving. The importance of early cardiac images is also reflected in patients, as through their analysis a differential diagnosis can be made in Parkinson's disease in just 25 minutes against the 4 hours now employed and revolutionizing a system in terms of lowering costs of the healthcare system and improving compliance of the patient.

CONCLUSIONS

The He/Me Ratio is almost as accurate as the widely used delayed 123I-mIBG imaging. This can reduce the burden of delayed imaging while preserving the diagnostic accuracy of the method. The importance of early cardiac images is also reflected in patients, as through their analysis a differential diagnosis can be made in Parkinson's disease in just 25 minutes against the 4 hours currently needed, lowering costs of the healthcare system and improving compliance of the patient.

ETHICS APPROVAL AND CONSENT TO PARTICIPATE

This study was approved by the ethic committee of Comitato Etico Università Sapienza di Roma, Rome, Italy - Ref number 3703

AVAILABILITY OF DATA AND MATERIALS:

All data generated or analysed during this study are available from the corresponding author on reasonable request.

HUMAN AND ANIMAL RIGHTS

This article does not contain any studies with animals performed by any of the authors. The study protocol was approved by the local ethics committee and conducted following the ethical standards laid down in the 1964 Declaration of Helsinki and its later amendments.

CONSENT FOR PUBLICATION

Not applicable.

FUNDING

None

CONFLICTS OF INTEREST

The authors have no conflicts of interest, financial or otherwise.

ACKNOWLEDGMENTS

Declared None

LIST OF ABBREVIATIONS

PD	=	Parkinson's Disease
123I-mIBG	=	Iodine-123-Metaiodobenzylguanidine
H/M	=	Heart-to-Mediastinum
He/Me	=	Early H/M
Hl/Ml	=	Late H/M
DLB	=	Dementia with Lewy bodies
RoIs	=	Region-of-Interests
FBP	=	Filtered-back-projection
ESS and LSS	=	Early and late summed scores
ROC	=	Receiver Operating Characteristic
MRD	=	Mean Relative Difference

REFERENCES

[1] Litvan, I.; MacIntyre, A.; Goetz, C.G.; Wenning, G.K.; Jellinger, K.; Verny, M.; Bartko, J.J.; Jankovic, J.; McKee, A.; Brandel, J.P.; Chaudhuri, K.R.; Lai, E.C.; D'Olhaberriague, L.; Pearce, R.K.B.; Agid, Y. Accuracy of the Clinical Diagnoses of Lewy Body Disease, Parkinson Disease, and Dementia With Lewy Bodies. Accuracy of the clinical diagnoses of Lewy body disease, Parkinson disease, and dementia with Lewy bodies: a clinicopathologic study. *Arch. Neurol.,* **1998**, *55*(7), 969-978. [http://dx.doi.org/10.1001/archneur.55.7.969] [PMID: 9678315]

[2] Gabilondo, I.; Llorens, V.; Rodriguez, T.; Fernández, M.; Concha, T.P.; Acera, M.; Tijero, B.; Murueta-Goyena, A.; Del Pino, R.; Cortés, J.; Gómez-Esteban, J.C. Myocardial MIBG scintigraphy in genetic Parkinson's disease as a model for Lewy body disorders. *Eur. J. Nucl. Med. Mol. Imaging,* **2019**, *46*(2), 376-384. [http://dx.doi.org/10.1007/s00259-018-4183-0] [PMID: 30324423]

[3] Okada, Y.; Shiraishi, M.; Nakamura, H.; Maki, F.; Sasaki, N.; Hasegawa, Y.; Sasaki, O.; Nakashima, Y. Usefulness of the combination of iodine-123-metaiodobenzylguanidine scintigraphy and iodine-123-ioflupane scintigraphy in new-onset Parkinson's disease. *Nucl. Med. Commun.,* **2018**, *39*(11), 983-988. [http://dx.doi.org/10.1097/MNM.0000000000000898] [PMID: 30180045]

[4] Orimo, S.; Ozawa, E.; Nakade, S.; Sugimoto, T.; Mizusawa, H. (123)I-metaiodobenzylguanidine myocardial scintigraphy in Parkinson's disease. *J. Neurol. Neurosurg. Psychiatry,* **1999**, *67*(2), 189-194. [http://dx.doi.org/10.1136/jnnp.67.2.189] [PMID: 10406987]

[5] Watanabe, H.; Ieda, T.; Katayama, T.; Takeda, A.; Aiba, I.; Doyu, M.; Hirayama, M.; Sobue, G. Cardiac (123)I-meta-iodobenzylguanidine (MIBG) uptake in dementia with Lewy bodies: comparison with Alzheimer's disease. *J. Neurol. Neurosurg. Psychiatry,* **2001**, *70*(6), 781-783. [http://dx.doi.org/10.1136/jnnp.70.6.781] [PMID: 11385013]

[6] Strano, S.; Fanciulli, A.; Rizzo, M.; Marinelli, P.; Palange, P.; Tiple, D.; De Vincentis, G.; Calcagnini, G.; Censi, F.; Meco, G.; Colosimo, C. Cardiovascular dysfunction in untreated Parkinson's disease: A multi-modality assessment. *J. Neurol. Sci.,* **2016**, *370*, 251-255. [http://dx.doi.org/10.1016/j.jns.2016.09.036] [PMID: 27772769]

[7] Bonanni, L.; Thomas, A.; Onofrj, M.; McKeith, I.G. Diagnosis

and management of dementia with Lewy bodies: third report of the DLB Consortium. *Neurology,* **2006**, *66*(9), 1455-1455. [http://dx.doi.org/10.1212/01.wnl.0000224698.67660.45] [PMID: 16682691]

[8] Treglia, G.; Stefanelli, A.; Cason, E.; Cocciolillo, F.; Di Giuda, D.; Giordano, A. Diagnostic performance of iodine-123-metaiodobenzylguanidine scintigraphy in differential diagnosis between Parkinson's disease and multiple-system atrophy: a systematic review and a meta-analysis. *Clin. Neurol. Neurosurg.,* **2011**, *113*(10), 823-829. [http://dx.doi.org/10.1016/j.clineuro.2011.09.004] [PMID: 21962800]

[9] Sawada, H.; Oeda, T.; Yamamoto, K.; Kitagawa, N.; Mizuta, E.; Hosokawa, R.; Ohba, M.; Nishio, R.; Yamakawa, K.; Takeuchi, H.; Shimohama, S.; Takahashi, R.; Kawamura, T. Diagnostic accuracy of cardiac metaiodobenzylguanidine scintigraphy in Parkinson disease. *Eur. J. Neurol.,* **2009**, *16*(2), 174-182. [http://dx.doi.org/10.1111/j.1468-1331.2008.02372.x] [PMID: 19146639]

[10] Maruyama, Y.; Yamada, T.; Murakami, K.; Kumano, R. Comparison of the diagnostic performance of H/M ratio between early and delayed phases for Lewy body disease. *Nucl. Med. Commun.,* **2015**, *36*(5), 477-480. [http://dx.doi.org/10.1097/MNM.0000000000000271] [PMID: 25714666]

[11] Sakamoto, F.; Shiraishi, S.; Tsuda, N.; Hashimoto, M.; Tomiguchi, S.; Ikeda, M.; Yamashita, Y. Diagnosis of dementia with Lewy bodies: can ^{123}I-IMP and ^{123}I-MIBG scintigraphy yield new core features? *Br. J. Radiol.,* **2017**, *90*(1070)20160156 [http://dx.doi.org/10.1259/bjr.20160156] [PMID: 27897064]

[12] Manabe, Y.; Inui, Y.; Toyama, H.; Kosaka, K. 123I-metaiodobenzylguanidine myocardial scintigraphy with early images alone is useful for the differential diagnosis of dementia with Lewy bodies. *Psychiatry Res. Neuroimaging,* **2017**, *261*, 75-79. [http://dx.doi.org/10.1016/j.pscychresns.2016.12.011] [PMID: 28152401]

[13] Gelb, D.J.; Oliver, E.; Gilman, S. Diagnostic criteria for Parkinson disease. *Arch. Neurol.,* **1999**, *56*(1), 33-39. [http://dx.doi.org/10.1001/archneur.56.1.33] [PMID: 9923759]

[14] Gilman, S.; Wenning, G.K.; Low, P.A.; Brooks, D.J.; Mathias, C.J.; Trojanowski, J.Q.; Wood, N.W.; Colosimo, C.; Dürr, A.; Fowler, C.J.; Kaufmann, H.; Klockgether, T.; Lees, A.; Poewe, W.; Quinn, N.; Revesz, T.; Robertson, D.; Sandroni, P.; Seppi, K.; Vidailhet, M. Second consensus statement on the diagnosis of multiple system atrophy. *Neurology,* **2008**, *71*(9), 670-676. [http://dx.doi.org/10.1212/01.wnl.0000324625.00404.15] [PMID: 18725592]

[15] De Vincentis, G.; Frantellizzi, V.; Fedele, F.; Farcomeni, A.; Scarparo, P.; Salvi, N.; Fegatelli, D.A.; Mancone, M.; Verschure, D.O.; Verberne, H.J. Role of cardiac ^{123}I-mIBG imaging in predicting arrhythmic events in stable chronic heart failure patients with an ICD. *J. Nucl. Cardiol.,* **2019**, *26*(4), 1188-1196. [http://dx.doi.org/10.1007/s12350-018-1258-z] [PMID: 29594915]

[16] Bewick, V.; Cheek, L.; Ball, J. Statistics review 13: receiver operating characteristic curves. *Crit. Care,* **2004**, *8*(6), 508-512. [http://dx.doi.org/10.1186/cc3000] [PMID: 15566624]

[17] Courbon, F.; Brefel-Courbon, C.; Thalamas, C.; Alibelli, M.J.; Berry, I.; Montastruc, J.L.; Rascol, O.; Senard, J.M. Cardiac MIBG scintigraphy is a sensitive tool for detecting cardiac sympathetic denervation in Parkinson's disease. *Mov. Disord.,* **2003**, *18*(8), 890-897. [http://dx.doi.org/10.1002/mds.10461] [PMID: 12889078]

[18] Orimo, S.; Amino, T.; Itoh, Y.; Takahashi, A.; Kojo, T.; Uchihara, T.; Tsuchiya, K.; Mori, F.; Wakabayashi, K.; Takahashi, H. Cardiac sympathetic denervation precedes neuronal loss in the sympathetic ganglia in Lewy body disease. *Acta Neuropathol.,* **2005**, *109*(6), 583-588. [http://dx.doi.org/10.1007/s00401-005-0995-7] [PMID: 15933869]

[19] Nakajima, K.; Verschure, D.O.; Okuda, K.; Verberne, H.J. Standardization of ^{123}I-*meta*-iodobenzylguanidine myocardial sympathetic activity imaging: phantom calibration and clinical applications. *Clin. Transl. Imaging,* **2017**, *5*(3), 255-263. [http://dx.doi.org/10.1007/s40336-017-0230-2] [PMID: 28596948]

[20] Brumberg, J.; Blazhenets, G.; Schröter, N.; Frings, L.; Jost, W.H.; Lapa, C.; Meyer, P.T. Imaging cardiac sympathetic innervation with MIBG: linear conversion of the heart-to-mediastinum ratio between different collimators. *EJNMMI Phys.,* **2019**, *6*(1), 12. [http://dx.doi.org/10.1186/s40658-019-0250-2] [PMID: 31338697]

[21] Flotats, A.; Carrió, I.; Agostini, D.; Le Guludec, D.; Marcassa, C.; Schäfers, M.; Somsen, G.A.; Unlu, M.; Verberne, H.J. EANM Cardiovascular Committee; European Council of Nuclear Cardiology. Proposal for standardization of 123I-metaiodobenzylguanidine (MIBG) cardiac sympathetic imaging by the EANM Cardiovascular Committee and the European Council of Nuclear Cardiology. *Eur. J. Nucl. Med. Mol. Imaging,* **2010**, *37*(9), 1802-1812. [http://dx.doi.org/10.1007/s00259-010-1491-4] [PMID: 20577740]

[22] Murakami, N.; Sako, W.; Haji, S.; Furukawa, T.; Otomi, Y.; Otsuka, H.; Izumi, Y.; Harada, M.; Kaji, R. Potential Utility of ^{123}I-MIBG Scintigraphy as a Predictor of Falls in Parkinson's Disease. *Front. Neurol.,* **2019**, *10*, 376. [http://dx.doi.org/10.3389/fneur.2019.00376] [PMID: 31031701]

[23] Nakajima, K.; Yamada, M. (123)I-Meta-iodobenzylguanidine Sympathetic Imaging: Standardization and Application to Neurological Diseases. *Chonnam Med. J.,* **2016**, *52*(3), 145-150. [http://dx.doi.org/10.4068/cmj.2016.52.3.145] [PMID: 27689024]

[24] Christensen, T.E.; Kjaer, A.; Hasbak, P. The clinical value of cardiac sympathetic imaging in heart failure. *Clin. Physiol. Funct. Imaging,* **2014**, *34*(3), 178-182. [http://dx.doi.org/10.1111/cpf.12091] [PMID: 24138454]

[25] Verschure, D.O.; Poel, E.; Nakajima, K.; Okuda, K.; van Eck-Smit, B.L.F.; Somsen, G.A.; Verberne, H.J. A European myocardial ^{123}I-mIBG cross-calibration phantom study. *J. Nucl. Cardiol.,* **2018**, *25*(4), 1191-1197. [http://dx.doi.org/10.1007/s12350-017-0782-6] [PMID: 28120154]